Pramana – J. Phys. (2021) 95:204
https://doi.org/10.1007/s12043-021-02240-8

Magnetoelectric composites of copper cobalt ferrite and lead zirconium titanate by screen printing method and their magnetoelectric properties

H V BHAVANA, SHAIK SABIRA BEGUM, A R VIJAYALAKSHMI and S S BELLAD*

Department of Physics, Materials Research Centre, Maharani Science College for Women, Bengaluru 560 001, India
*Corresponding author. E-mail: ssbellad@rediffmail.com

MS received 11 April 2021; revised 20 July 2021; accepted 9 August 2021

Abstract. Magnetoelectric composites of the ferrite phase $Cu_{1-x}Co_xFe_2O_4$ (where $x = 0, 0.1, 0.2, 0.3, 0.4, 0.5$) and the ferroelectric phase $PbZr_{0.58}Ti_{0.42}O_3$ were synthesised by conventional solid-state reaction method. X-ray diffraction studies reveal the coexistence of the ferrite phase with cubic spinel structure and ferroelectric phase with perovskite structure. Ferrite/PZT/ferrite, PZT/ferrite/PZT trilayered structures are fabricated using screen printing technique. The variation of dielectric constant and loss tangent in the frequency range 100 Hz to 5 MHz and with temperature at a fixed frequency of 1 kHz were studied. Dielectric properties are explained based on dielectric relaxation. At room temperature, AC resistivity decreases with increase in frequency which is due to the hopping frequency of charge carriers at equivalent ionic sites. Conductivity measurements confirm the small polaron hopping mechanism. Transverse ME voltage coefficient (α_{E31}) increases gradually attaining the maximum value at 400 Oe and then decreases beyond that with respect to the applied DC bias magnetic field. The variation of α_{E31} with applied DC external bias magnetic field was explained based on the domain growth and reorientation of domains with the applied magnetic field.

Keywords. ME composites; ferrites; ferroelectrics; dielectrics; screen printing.

PACS Nos **01.40.Fk; 61.05.cp; 68.55.A-; 68.65.Ac**

1. Introduction

Multiferroic magnetoelectric materials are a new class of materials which find applications in the field of sensors, microwave field, current measurement, switches, integral optics, fibre communication technology, isolators, modulators, waveguides, four-state memory devices etc. [1–6]. The research on magnetoelectric composites started with research on single-phase multiferroics. But the magnitude of the observed magnetoelectric effect and their working temperatures are very low in these materials and hence they could not find any reasonable practical applications, whereas in composite multiferroics, a magnetic phase with high magnetostriction coefficient and ferroelectric phase with high piezoelectric coefficient are mixed in a suitable proportion. This leads to an enormous increase in the magnitude of the magnetoelectric effect (ME). Thus, the ME effect is referred to as the product of the magnetostrictive and piezoelectric properties of the magnetic and electric phases. When magnetic field is applied to an ME composite, magnetostriction takes place along with the changes in domain structure. This leads to some strain which results in dielectric polarisation in ferroelectric phase and is referred to as direct ME effect. The direct ME effects are potentially useful in magnetic field sensing, novel magnetic recording read heads, current measurement probes for high power electric transmission systems and for energy harvesting [7]. In a similar manner, if the electric field is applied to ME composites, magnetisation is produced in the magnetic phase which is called the converse ME effect. The converse ME effects are useful for the electric field control of magnetic properties thereby reducing the size of the device which is of great importance [8,9].

Due to the low resistivity of ferrites, high leakage current is produced in the bulk composites yielding lower values of ME coefficient (α) than the values from the theoretical calculations. But this problem can be avoided

Published online: 27 November 2021

by fabricating layered composites which have comparatively high resistivity and negligible leakage current [10]. Screen printing is one of the techniques used for depositing layered composites which is an easy, low cost and highly preferred method to get thick films of any shape and size. Many reports have been found in the literature where screen printing method was used for the deposition of films of ME composites [11–15]. There are many research reports in the literature on bulk ME composites [16–20]. However, no reports have been found on $Cu_{1-x}Co_xFe_2O_4$:$PbZr_{0.58}Ti_{0.42}O_3$ layered composites in the literature. Therefore, in the present study we report on the dielectric and magnetoelectric properties of these trilayered composites fabricated using screen printing method.

2. Experimental details

2.1 *Synthesis of $Cu_{1-x}Co_xFe_2O_4$ and $PbZr_{0.58}Ti_{0.42}O_3$ powders*

Magnetoelectric composites were prepared by conventional solid-state reaction method. Ferrite phase $Cu_{1-x}Co_xFe_2O_4$ (where $x = 0, 0.1, 0.2, 0.3, 0.4, 0.5$) was prepared by taking AR grade oxides of CuO, Co_3O_4, Fe_2O_3 and ferroelectric phase $PbZr_{0.58}Ti_{0.42}O_3$ was prepared by taking AR grade oxides PbO, ZrO_2, TiO_2 powders separately in stoichiometric proportions. Starting ingredients were mixed in acetone medium and ground to a fine powder in agate mortar. The presintering was done at 600°C and 650°C for 6 h separately for ferrite and ferroelectric phases respectively. The presintered powder was again ground to a fine powder and final sintering was done at 900°C for 12 h for both the phases.

2.2 *Thick film deposition*

Deposition of thick films (0.33 mm thick) was done by using screen printing method. Ferrite and ferroelectric powders were separately mixed with 10% ethyl cellulose solution (ethyl cellulose+terpineol) to get the paste. The fabrication of tri-layered ME composites was done as follows: First layer of the ferrite phase was deposited on the conducting side of the fluorine-doped tin oxide (FTO) substrate by squeezing the paste through the mesh screen and set aside for drying at room temperature for about 12 h. After drying, second layer of lead zirconium titanate (PZT) was deposited over the first layer in a similar manner. Third layer of the ferrite phase was also deposited over the second layer of PZT to complete the fabrication. Lastly, the fabricated tri -layered thick films were heated on a hot plate for about 300°C for 30 min to get ME composites. In a similar manner, the PZT/ferrite/PZT layered thick film composites were also fabricated. The fabricated structures are shown in figure 1.

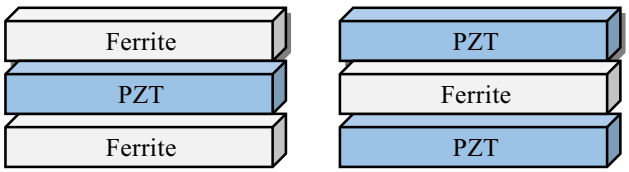

Figure 1. Fabrication of thick film structures.

The dielectric properties were measured at room temperature as a function of frequency in the range 100 Hz to 5 MHz and at a fixed frequency (1 kHz) as a function of temperature by using the impedance analyser Wayne Kerr 6500B. The direct transverse magnetoelectric coefficient (α_{E31}) was calculated using the relation $\alpha_{E31} = V_{ME}/(t \times H_{AC})$ where V_{ME} is the induced voltage, t is the thickness of the film and H_{AC} is the AC field applied. The electromagnets which produce DC magnetic field (H_{DC}) and a pair of Helmholtz coils which produces AC magnetic field (H_{AC}) were placed coaxially. The tri-layered composite structure was placed at the middle of the Helmholtz coils on their axis in L-T (longitudinally magnetised and transversely polled) mode so that H_{DC} and H_{AC} are parallel to each other and to the plane of the sample. The ME voltage was measured perpendicular to the sample plane with the help of the lock-in amplifier. The AC magnetic field was kept constant (1 Oe), and the DC magnetic field was varied from 0 to 800 Oe.

3. Results and discussions

X-ray diffraction studies were carried out on the ferrite as well as ferroelectric powders to check the completion of solid-state reaction process. Figures 2 and 3 show the representative XRD patterns of both ferrite and ferroelectric phases respectively. The cubic spinel structure of the ferrite phase and the tetragonal perovskite structure of the ferroelectric phase can be clearly seen in figures 2 and 3 respectively [21]. The dominant high intensity peaks (311) of the ferrite phase and (101) of the ferroelectric phase are rightly positioned in their usual place.

The variations of dielectric constant as a function of frequency in ferrite/PZT/ferrite and PZT/ferrite/PZT are shown in figure 4. It is observed from figure 4 that in both the structures, the dielectric constant

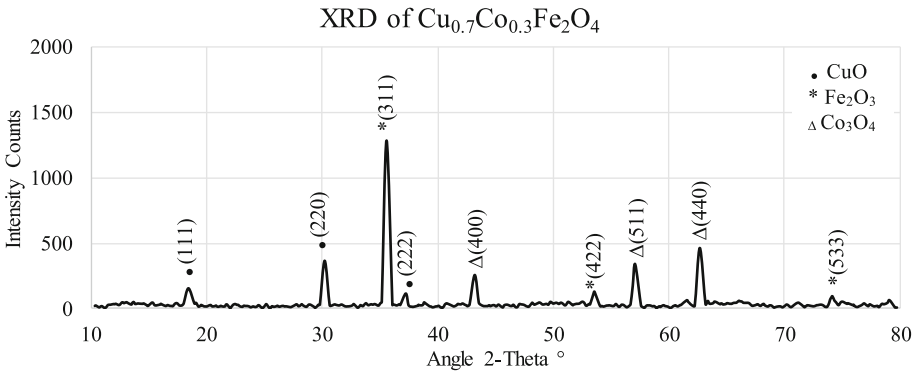

Figure 2. XRD pattern of $Cu_{0.7}Co_{0.3}Fe_2O_4$.

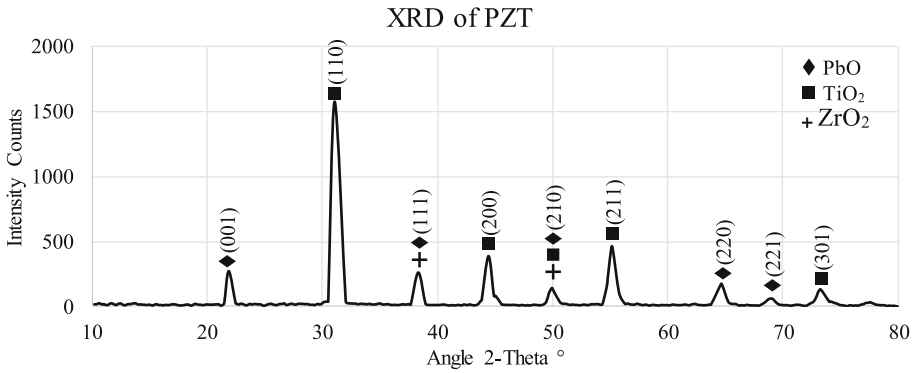

Figure 3. XRD pattern of PZT.

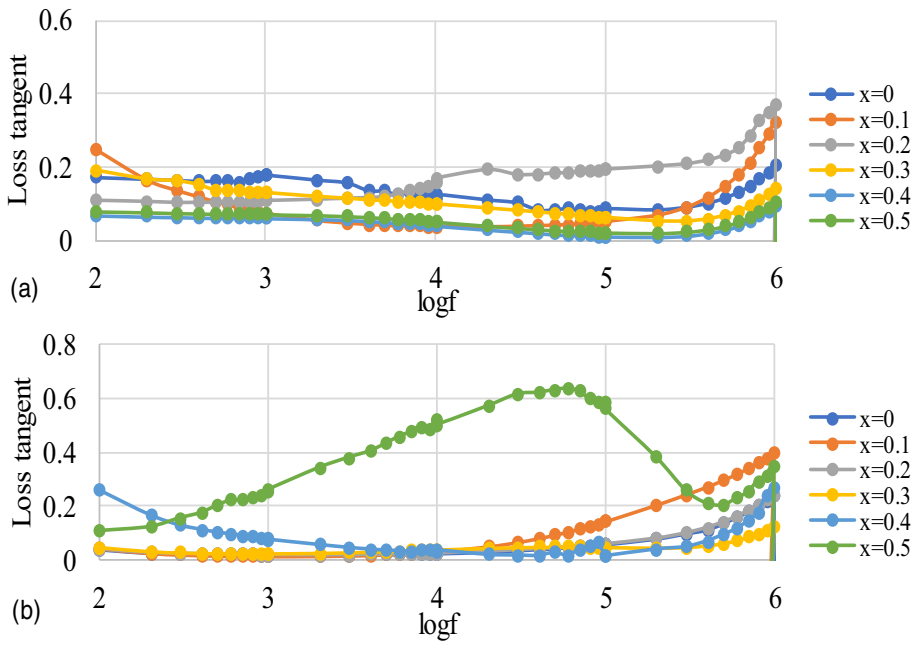

Figure 4. Variation of loss tangent with frequency for (**a**) $Cu_{1-x}Co_xFe_2O_4/PZT/Cu_{1-x}Co_xFe_2O_4$ and (**b**) $PZT/Cu_{1-x}Co_xFe_2O_4/PZT$ ($x = 0, 0.1, 0.2, 0.3, 0.4, 0.5$) thick films at room temperature.

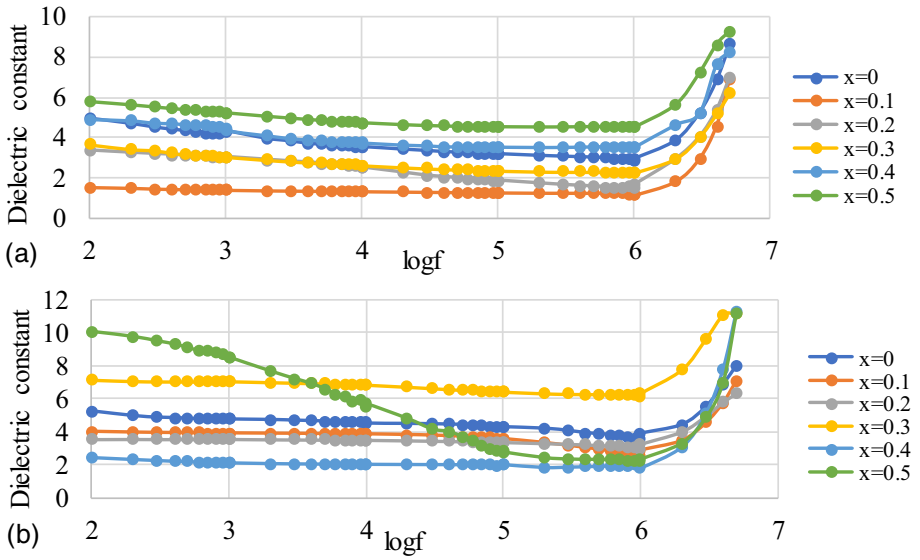

Figure 5. Variation of dielectric constant with frequency for (**a**) $Cu_{1-x}Co_xFe_2O_4/PZT/Cu_{1-x}Co_xFe_2O_4$ and (**b**) $PZT/Cu_{1-x}Co_xFe_2O_4/PZT$ ($x = 0, 0.1, 0.2, 0.3, 0.4, 0.5$) thick films at room temperature.

almost remains flat up to 1 MHz of the applied frequency and beyond this frequency all the samples tend to show an absorption peak. However, in the PZT/ferrite/PZT structure, for $x = 0.5$ the sample showed normal dielectric behaviour up to 1 MHz. The dielectric dispersion observed at low frequency is due to Maxwell–Wagner-type interfacial polarisation which is in agreement with Koop phenomenological theory [22]. Variation of dielectric constant with frequency was generally explained on the basis of the dielectric relaxation process which was the consequence of space-charge polarisation in the samples. Space-charge polarisation arises due to the inhomogeneities in the films, i.e., impurities, porosity and grain structure. The absorption peak which can be observed beyond 1 MHz of applied frequency may be due to the resonance phenomenon which occurs between hopping frequency of charge carriers at equivalent ionic sites and applied frequency [23]. The flatness in the curves of dielectric constant vs. frequency plots can be due to the weak dielectric relaxation process [23].

The variations of loss tangent with frequency for both tri-layered structures are shown in figure 5. Loss tangent and dielectric constant show the same behaviour. This trend was well established in many dielectric systems [22–24]. The normal dielectric behaviour was observed below 1 MHz for sample $x = 0.5$ which shows the enhanced dielectric relaxation processes.

Variations of dielectric constant with temperature at 1 kHz were studied for tri-layered structures and shown in figure 6. It is seen from the figure that for the PZT/ferrite/PZT structure, the dielectric constant remains constant in the whole range of temperature studied (300 to 450 K) and in the ferrite/PZT/ferrite structure, the dielectric constant remains constant up to 400 K and beyond that temperature, it tends to increase with further increase in temperature. In many magnetoelectric bulk composites, the dielectric constant has increased very slowly up to 400 K and beyond that it has increased abruptly [18–20]. This abrupt increase in dielectric constant with temperature was attributed to the enhancement in hopping frequency of electrons between Fe^{2+} and Fe^{3+} ions due to the increase in thermal energy. Electron hopping results in the local displacement in the direction of applied electric field which causes dielectric polarisation in ferrite leading to an increase in dielectric constant. Even, a peak was observed at phase transition of the material from ferromagnetic to paramagnetic state [18,19], whereas in the present study it is very clear from figure 6, that in the PZT/ferrite/PZT structure all the curves are flat in the temperature range studied and in ferrite/PZT/ferrite, the curves are flat up to 400 K and beyond that there is an increasing trend. This flatness in the curves below 400 K indicates that the hopping frequency of electrons in this temperature range is not thermally activated in both the structures [24].

Variations of AC resistivity with frequency for both the tri-layered structures are shown in figure 7. From figure 7 it can be seen that with increase in applied frequency, resistivity decreases up to 10 kHz and beyond that value it attains saturation. The dispersion observed in resistivity at low frequency can be explained on similar lines given for dielectric dispersion at low frequency

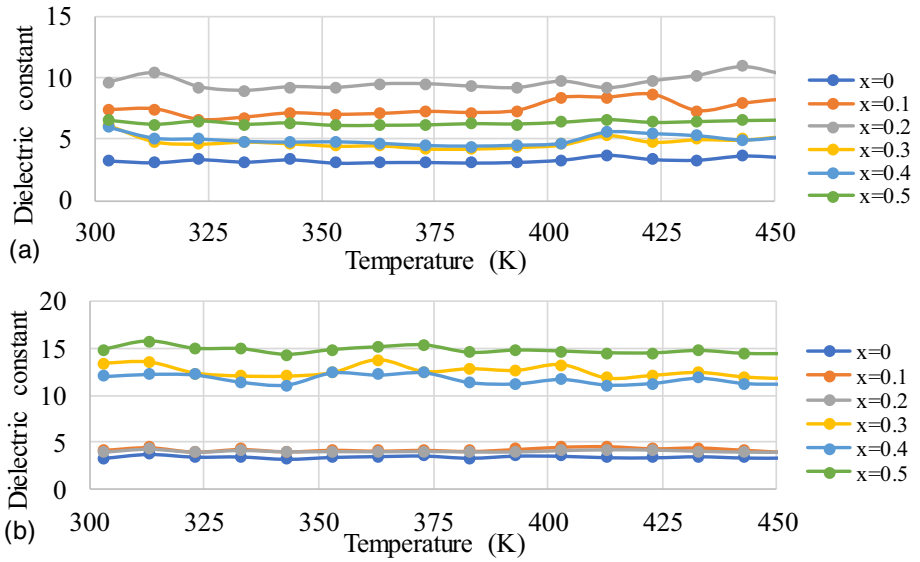

Figure 6. Variation of dielectric constant with temperature for (**a**) $Cu_{1-x}Co_xFe_2O_4/PZT/Cu_{1-x}Co_xFe_2O_4$ and (**b**) $PZT/Cu_{1-x}Co_xFe_2O_4/PZT$ ($x = 0, 0.1, 0.2, 0.3, 0.4, 0.5$) thick films.

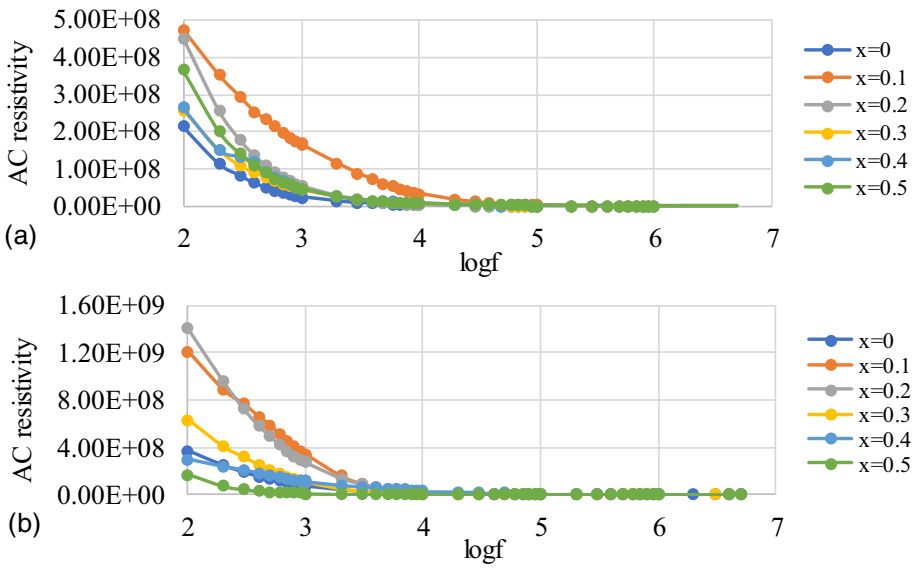

Figure 7. Variation of AC resistivity with frequency for (**a**) $Cu_{1-x}Co_xFe_2O_4/PZT/Cu_{1-x}Co_xFe_2O_4$ and (**b**) $PZT/Cu_{1-x}Co_xFe_2O_4/PZT$ ($x = 0, 0.1, 0.2, 0.3, 0.4, 0.5$) thick films at room temperature.

[23]. The decrease in resistivity with increase in frequency is due to the increase in hopping frequency of electrons between the equivalent ionic sites in the lattice. The saturation beyond 10 kHz is attributed to the fact that the hopping frequency of electrons does not follow the applied frequency anymore [23].

From the AC resistivity measurement data, AC conductivity can be calculated and using that data log(conductivity) vs. log(ω^2) graphs are plotted in figure 8. The linearity in the curves of all the samples reveal that the conduction in the studied samples is due to the hopping of small polarons [25].

The variation of ME voltage coefficient with respect to the applied DC bias magnetic field for both the structures are shown in figure 9. In both the structures, as the applied DC magnetic field increases, the transverse ME voltage coefficient α_{E31} gradually increases and reaches a peak when the applied magnetic field is 400 Oe and then decreases gradually beyond this field. The ME voltage coefficient reaches saturation value beyond 600 Oe in both the structures. The value of α_{E31} depends on the resistivity of the ferrite phase, magnetostriction coefficient of the ferrite phase, the type of connectivity

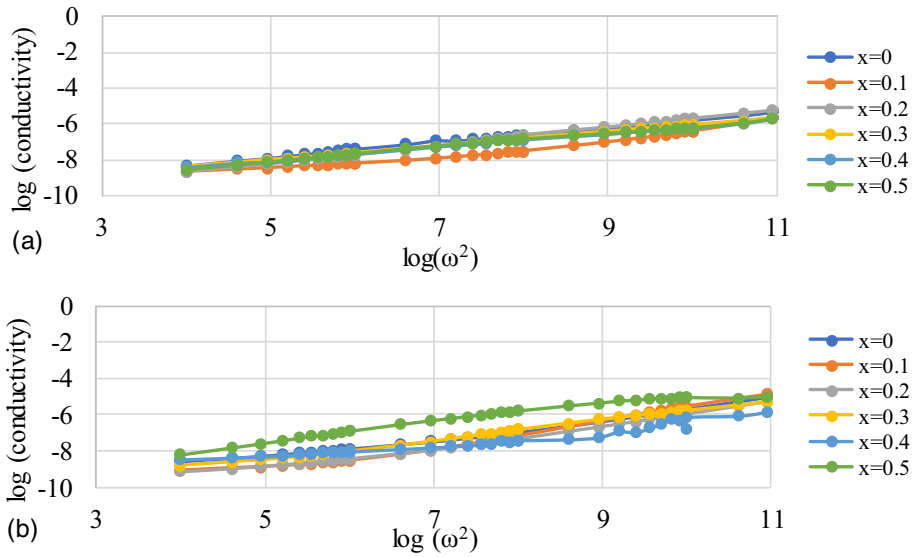

Figure 8. Variation of AC conductivity with frequency for (**a**) $Cu_{1-x}Co_xFe_2O_4/PZT/Cu_{1-x}Co_xFe_2O_4$ and (**b**) $PZT/Cu_{1-x}Co_xFe_2O_4/PZT$ ($x = 0, 0.1, 0.2, 0.3, 0.4, 0.5$) thick films at room temperature.

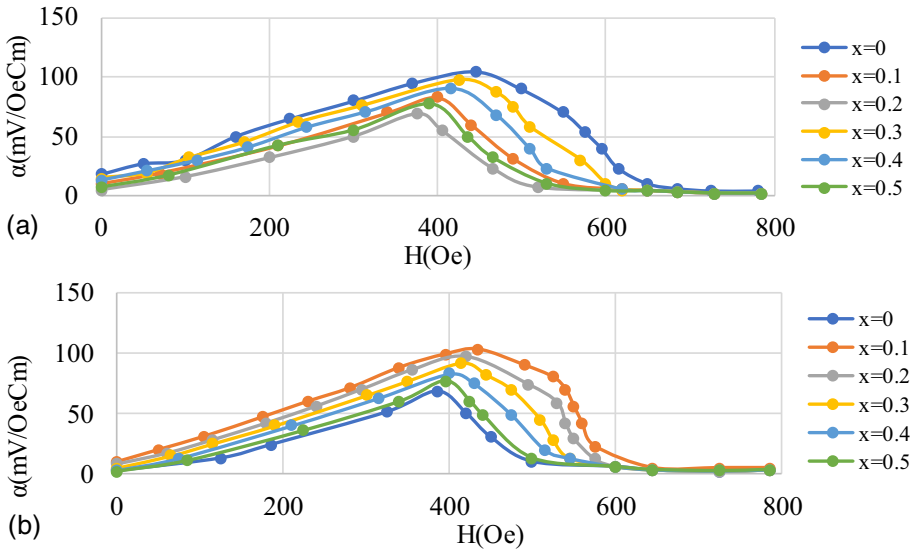

Figure 9. Variation of ME coefficient with DC bias field for (**a**) $Cu_{1-x}Co_xFe_2O_4/PZT/Cu_{1-x}Co_xFe_2O_4$ and (**b**) $PZT/Cu_{1-x}Co_xFe_2O_4/PZT$ ($x = 0, 0.1, 0.2, 0.3, 0.4, 0.5$) thick films.

between the ferrite and ferroelectric phases. The resistivity of the ferrite phase is generally found to be less than that of the ferroelectric phase. Therefore, if the resistivity of the ferrite phase is less, then there is a chance of flowing of leakage current between the two phases, thereby accumulation of charges is hindered, leading to the lowering of the ME coefficient. The magnetostriction coefficient of the ferrite phase decides how the material is responding to the applied magnetic field. Higher the value of magnetostriction, higher will be the domain wall movements, and this leads to higher magnitudes of the stress developed on the ferroelectric phase leading to development of higher values of ME voltage. The connectivity between the two phases also plays a vital role in fetching the ME voltage coefficient. The 0–3 connectivity which exists when a nanopowder of magnetic phase was embedded in the matrix of ferroelectric phase as in case of bulk ME composites has led to the failure of ME composites in achieving good values of α_{E31}. The reason for this was that, this type of

connectivity cannot produce higher values of stresses on the ferroelectric phase. In the case of 1–3 connectivity, where the nanorods of the magnetic phase are embedded in the matrix of the ferroelectric phase, α_{E31} values again could not improve for the same reason. The 2–2 type of connectivity exists when one type of thin/thick layer of one phase is coated over another layer of the other phase. This type of connectivity can produce good values of α_{E31} as the conditions for good values of α_{E31} are met. In the present study, we have developed 2–2 connectivity between the ferrite and ferroelectric layers. This has fetched us good values of α_{E31} compared to bulk composites [18–20].

As the applied magnetic field increases, the domains in the magnetic phase which are in the direction of the applied magnetic field starts growing and other domains which are in other direction starts shrinking. As the applied magnetic field increases further, even the reorientation of the domains in the direction of the applied magnetic field takes place. When the applied field is 400 Oe, this mechanism is at its maximum leading to the maximum value of α_{E31}. Beyond 400 Oe, the growth of the magnetic domains saturates and all the domains become stable and hence the stress developed over the ferroelectric phase start releasing for further increase of external field leading to the decrease of α_{E31} [26].

4. Conclusion

The tri-layered ME composites having the ferrite phase $Cu_{1-x}Co_xFe_2O_4$ where $x = 0, 0.1, 0.2, 0.3, 0.4, 0.5$ and ferroelectric phase $PbZr_{0.58}Ti_{0.42}O_3$ are synthesised by conventional solid-state reaction method. The XRD study revealed the coexistence of cubic spinal structure of the ferrite phase and perovskite structures of the ferroelectric phase. Tri-layered thick film structures were fabricated successfully by screen printing technique. Dielectric constant and loss tangent remain almost constant up to 1 MHz of applied frequency and beyond this range tend to show the absorption peak. The dispersion observed at the low frequency range is explained based on the space-charge polarisation. Dielectric constant does not vary with the studied temperature range, indicating that thermally generated electron hopping phenomenon is absent. Conductivity measurements established the presence of small polaron hopping mechanism. AC resistivity decreases with increase in frequency due to increase in hopping frequency of charge carriers at equivalent ionic sites. Higher values of α_{E31} observed in the present study is attributed to the 2–2 connectivity of the tri-layers which favours the requirements for good ME effect. In both the structures, as the applied DC magnetic field increases, the transverse ME voltage coefficient α_{E31} gradually increases and reaches a peak value at 400 Oe magnetic field and then decreases gradually beyond this field.

Acknowledgements

The authors are thankful to Dr G Ram Gopal, Principal, Dr G Sriprakash, HoD and Dr N Hanumanth Raju, Department of Physics, Maharani Science College for Women, Maharani Cluster University, Bengaluru for their help and support during this work. They also thank Dept. of Science and Technology (DST), Govt. of India, for supporting FIST Programme in our college/university.

References

[1] D K Pradhan, R N P Chowdhury and T K Nath, *Appl. Nanosci.* **2**, 261 (2012)
[2] Nidhi Adhlalcha and Kanhaiya Lal Yadav, *Smart Mater. Struct.* **21**, 115021 (2012)
[3] Ajay Singh, Shivani Suri, Parveen Kumar, Balwinder Kaur, A K Thakur and Vishal Singh, *J. Alloys Compd* **764**, 599 (2018)
[4] Sanjay Kumar Upadhyay and V Raghavnedra Reddy, *J. Appl. Phys.* **113**, 114107 (2013)
[5] Rishikesh Pandeya, Uma Shankar, Sher Singh Meena and Akhilesh Kumar Singh, *Ceram. Int.* **45**, 23013 (2019)
[6] M R Hassan, Md Sarowar Hossain, M A Hakim, M A Matin, M N I Khan and S S Sikder, *Results Phys.* **26**, 104340 (2021)
[7] N A Pertsev, H Kohlstedt and B Dkhil, *Phys. Rev. B* **80**, 054102 (2009)
[8] Y H Tang, X M Chen, Y J Li and X H Zheng, *Mater. Sci. Eng. B* **116**, 150(2005)
[9] Jungho Ryu, Alfredo Vázquez Carazo, Kenji Uchino and Hyoun-Ee Kim, *Jpn. J. Appl. Phys.* **40**, 4948 (2001)
[10] G Srinivasan and R Hayes, *Solid State Commun.* **128**, 261 (2003)
[11] A A Bush, V Ya Shkuratov, I A Chernykh and Y K Fetisov, *Tech. Phys.* **55**, 387 (2010)
[12] S A Waghuley, S M Yenorkar, S S Yawale and S P Yawale, *Sensors Transducers J.* **79**, 1180 (2007)
[13] G H Jain and L A Patil, *Bull. Mater. Sci.* **29**, 403 (2006)
[14] A V Patil, C G Dighavkar, S K Sonawane, S J Patil and R Y Borse, *Optoelectron. Biomed. Mater.* **1**, 226 (2009)
[15] R A Dorey, R W Whatmore, S P Beeby, R N Torah and N M White, *Integ. Ferroelectron.* **54**, 651 (2003)
[16] N M Burange, R K Pinjari and B A Aldar, *IOSR J. Appl. Chem.* **7**, 60 (2014)
[17] Sanjay Kumar Upadhyay, V Raghavendra Reddy and N Lakshmi, *J. Asian Ceramic Soc.* **1**, 346 (2013)

[18] Bablu Chandra Das and A K M Akther Hossain, *J. Alloys Compd* **867**, 159068 (2021)
[19] S L Kadam, K K Patankar, V L Mathe, M B Kothale, R B Kale and B K Chougule, *Mater. Chem. Phys.* **78**, 684 (2003)
[20] Pankhuri Bansal, Manoj Kumar, Rajat Syal, Arun Kumar Singh and Sanjeev Kumar, *J. Mater. Sci: Mater. Electron.* **32**, 17512 (2021)
[21] V V Shvartsman, F Alawneh, P Borisov, D Kozodaev and D C Lupascu, *Smart Mater. Struct.* **20**, 075006 (2011)
[22] S A Lokare, R S Devan, D R Patil and B K Chougule, *J. Mater. Sci.: Mater. Electron.* **18**, 1211 (2007)
[23] S U Durgadsimi, S S Chougule, B K Chougule, C H Bhosale and S S Bellad, *Mater. Chem. Phys.* **131**, 199 (2011)
[24] S A Lokare, D R Patil and B K Chougule, *J. Alloys Compd* **453**, 58 (2008)
[25] R P Mahajan, K K Patankar, M B Kothale and S A Patil, *Bull. Mater. Sci.* **23**, 273 (2000)
[26] A A Timopheev, J V Vidal, A L Kholkin and N A Sobolev, *J. Appl. Phys*. **114**, 044102 (2013)